



**HAL**  
open science

# Extensive investigation of the mechanical properties of a Chooz A internal component

J. Hure, B. Tanguy, C. Ritter, S. Bourganel, F. Sefta

## ► To cite this version:

J. Hure, B. Tanguy, C. Ritter, S. Bourganel, F. Sefta. Extensive investigation of the mechanical properties of a Chooz A internal component. Fontevraud 9, Sep 2018, Avignon, France. cea-02338571

**HAL Id: cea-02338571**

**<https://cea.hal.science/cea-02338571>**

Submitted on 24 Feb 2020

**HAL** is a multi-disciplinary open access archive for the deposit and dissemination of scientific research documents, whether they are published or not. The documents may come from teaching and research institutions in France or abroad, or from public or private research centers.

L'archive ouverte pluridisciplinaire **HAL**, est destinée au dépôt et à la diffusion de documents scientifiques de niveau recherche, publiés ou non, émanant des établissements d'enseignement et de recherche français ou étrangers, des laboratoires publics ou privés.

# Extensive investigation of the mechanical properties of a Chooz A internal component

J. Hure<sup>1\*</sup>, B. Tanguy<sup>1</sup>, C. Ritter<sup>1</sup>, S. Bourganel<sup>2</sup>, F. Sefta<sup>3</sup>

<sup>1</sup> CEA Saclay, Université Paris-Saclay, DEN, Service d'Etudes des Matériaux Irradiés, 91191 Gif-sur-Yvette, France

<sup>2</sup> CEA Saclay, Université Paris-Saclay, DEN, Service d'Etudes des Réacteurs et de Mathématiques Appliquées, 91191 Gif-sur-Yvette, France

<sup>3</sup> EDF Lab Les Renardières, F-77818 Moret-sur-Loing, France

\*Main Author, E-mail: jeremy.hure@cea.fr

**Keywords:** *Austenitic stainless steel, Tensile properties, Toughness, Fracture mechanisms*

## Introduction

In PWR's, internals made of austenitic stainless steels (Cold Worked (CW) 316 austenitic steels for bolts, 308 for welds and Solution Annealed (SA) 304 for baffle plates, former and core barrel) are subjected to irradiation embrittlement with doses that will reach up to 80 dpa locally after 40 years of operation at temperatures between 280°C and 380°C. The irradiation exposure alters the nanostructure and so consequently do the mechanical properties of stainless steels: it increases the yield strength, decreases ductility and promotes plastic instabilities. These evolutions of mechanical properties with irradiation may have dramatic consequences on the fracture properties: CW316 and SA304 have been shown to become sensitive to Stress Corrosion Cracking in PWR environment, a phenomenon known as IASCC [1] affecting baffle-to-former bolts. Moreover, neutron irradiation at low temperature generally causes a strong decrease of fracture toughness. Austenitic stainless steels are characterized by their ductility and stable crack propagation. However, fracture toughness (as measured by the J-integral at the onset of crack propagation  $J_{ic}$  [2]) may decrease by a factor up to ten after few dpa of irradiation, with a reduced stable crack propagation, or even brittle-like unstable crack propagation for the highest irradiation levels. Detailed reviews of the available experimental data have been provided regarding the evolution of tensile properties and fracture toughness of austenitic stainless steels with irradiation [1,2,3] at temperatures about 330°C, discussing the effects of materials, irradiation conditions (temperature, neutron spectrum) and providing correlations or bounding curves for the evolution of these properties with irradiation. Most of the data, especially for high doses, comes from irradiation in fast-spectrum reactors, while the remaining have been obtained from materials retrieved from commercial LWR's or irradiated in mixed spectrum Materials Testing Reactors (MTR). For tensile properties, both subsets of data have been shown to follow the same trends with respect to the saturation of yield stress and mechanical strength with irradiation [2]. However, few data available from LWR's are above the data from fast reactors. Similarly, for fracture toughness tests, only limited data are available from LWR irradiated materials, limited to doses less than about 10dpa for 304, and seems to fall below the bounding curves established from fast-reactors irradiation. More experimental data - tensile properties and fracture toughness - from austenitic stainless steels irradiated in LWR conditions are thus required to provide reliable predictions of the evolution of tensile properties and fracture toughness with irradiation in LWR conditions. In addition, fracture mechanisms of irradiated austenitic stainless steels depend on irradiation conditions (dose and temperature) and test conditions, as reviewed recently in [4]. Void growth to coalescence is observed at the unirradiated state and appears to remain dominant at 330°C for irradiated materials in LWR conditions, but intergranular fracture is also reported at lower test temperature or in aqueous environment (IASCC). At higher irradiation temperature, different fracture mechanisms have been described, such as channel fracture or nano-void growth to coalescence, which imply to treat with great caution the fracture toughness data obtained from high temperature irradiation to LWR conditions. Finally, a deep understanding of the fracture mechanisms will be required to go beyond correlation laws and to provide physically based fracture models for irradiated stainless steels.

The aim of this study is thus to provide tensile properties, fracture toughness estimation and observations of fracture mechanisms of a 304 austenitic stainless steel irradiated at high doses (>10dpa) in PWR conditions. First, the material and irradiation conditions are described as well as the machining of the tensile and fracture toughness samples. Tensile properties and fracture toughness properties are then reported, with Scanning Electron Microscope (SEM) observations of the fracture mechanisms. Results are finally discussed with respect to available literature data.

## Material and Samples preparation

This study is based on a component from the lower internals (Fig. 1a) of the French decommissioned PWR Chooz A operated for 24 years (between 1967 and 1991) [5]. Chooz A was the first PWR reactor built in France, with an electric power of 305MW. Unlike newer PWR designs, baffles made of 304 austenitic stainless steel (Fig. 1a) separated fuel assemblies at the periphery of the core. The chemical composition of the material is given in Tab. 1. The irradiation temperature of the component used in this study ranges from 290°C to 330°C, and doses up to 38dpa were estimated based on neutronic computations. One of these baffles was cut into pieces as sketched on Fig. 1b.

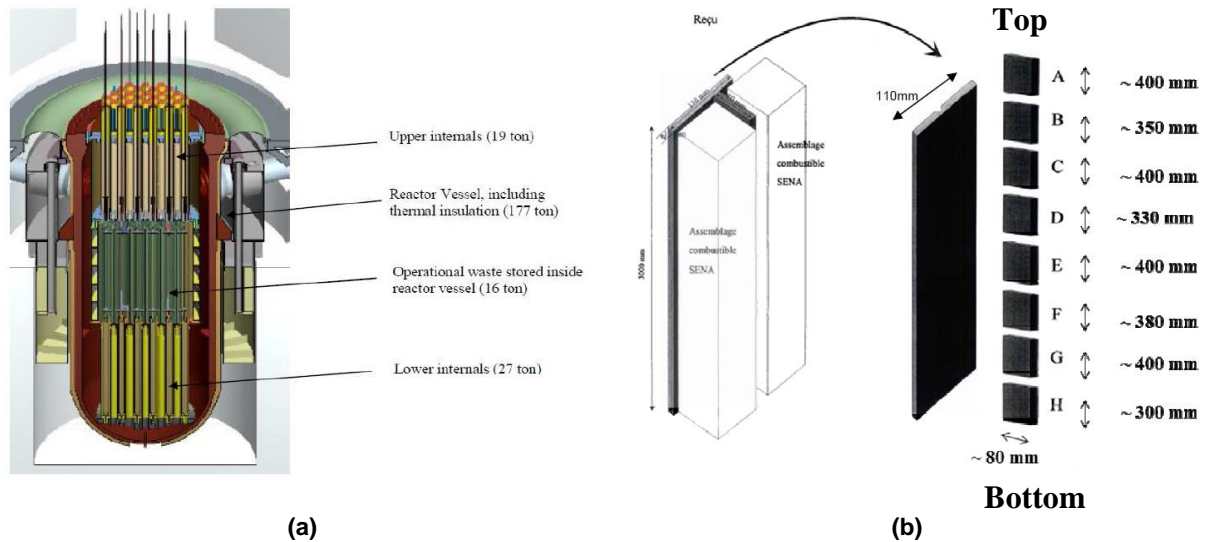


Figure 1: (a) Chooz A Reactor Pressure Vessel [6], (b) Location of the component used in this study

C	S	P	B	Mo	Co	Si	Mn	Cr	Ni	V	Nb	Cu	Ti
0.06	0.003	0.011	<0.0005	0.02	0.034	0.78	0.96	18.6	9.3	0.099	<0.02	0.089	<0.003

Table 1: Chemical composition (%wt) of 304 austenitic stainless steel

Blocks A, C and H were cut into sub-blocks used to machine tensile and fracture toughness samples. Fig. 2 indicates the location of the sub-blocks (referred to as CEA-1A,-1H,-1C,-2C,-3C), as well as evaluations of irradiation temperature and dose. For the latter, two methodologies were used to compute the dpa levels that differs especially for the block A. Additional evaluation of the dose is currently in progress, based on activity ( $^{60}\text{Co}$ ) measurements at precise locations along the blocks and neutronic computations, and results will be reported elsewhere. In the following, dose reported for the samples corresponds to the evaluation denoted (W) on Fig. 2, assuming linear dose gradient along the block due to their relatively small sizes. Ten flat tensile specimens were machined with gage lengths aligned with the top-bottom axis of the baffle through wire-cut electrical discharge machining and conventional milling. Two geometries are considered: the first one is shown on Fig. 3a and referred to as M1, the second one is homothetic to M1 of ratio 2, and is referred to as M2. Seven fracture toughness 1/2T Compact Tension (CT) specimens were also machined through wire-cut electrical discharge machining and conventional milling for the pin holes and side grooves (Fig. 3b). All samples machining, mechanical testing and SEM observations reported hereafter were performed at the LECI hot cells facility (CEA Saclay).

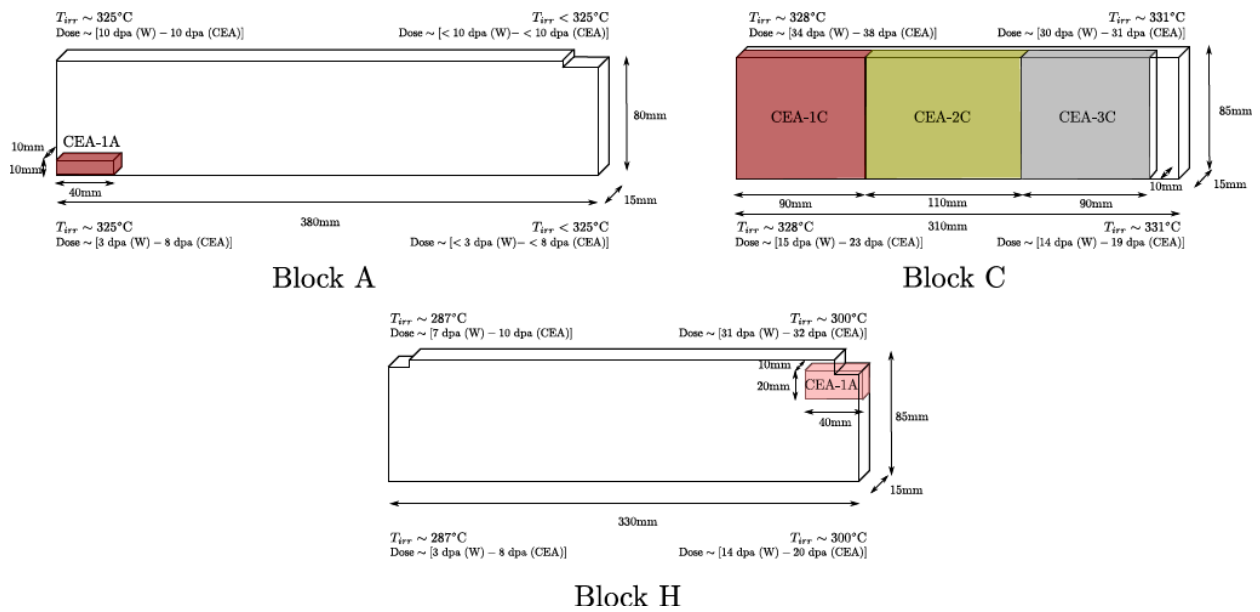


Figure 2: Location of the sub-blocks (CEA-1A,-1H,-1C,-2C,-3C) used to machine the tensile and fracture toughness samples. Irradiation temperature and dose evaluations. Right (resp. left) part of each block corresponds to top (resp. bottom) part of the baffle. No estimation of dose gradient along the (15mm) thickness is available.

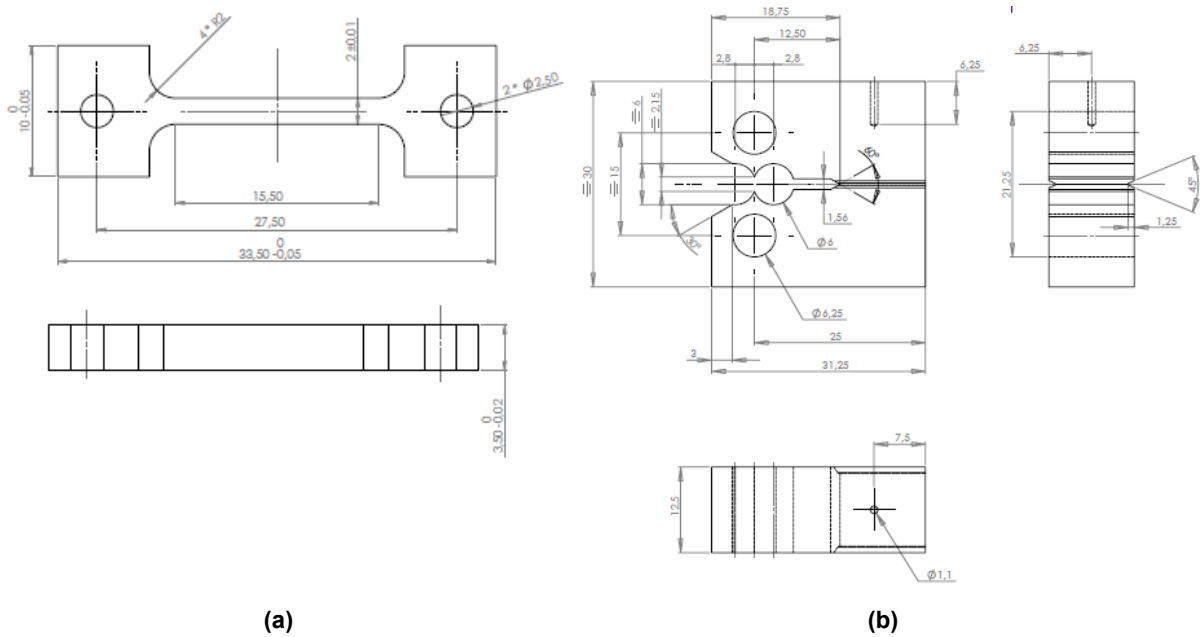


Figure 3: Samples geometry: (a) Tensile specimen (M1), (b) 1/2T Compact-Tension specimen (Dimensions in mm)

## Tensile properties

In order to evaluate the conventional tensile properties as a function of irradiation dose and temperature, tensile tests were performed on specimens shown in Fig. 3a at both room temperature and 330°C. Universal testing machines in hot cells were used under displacement control at a mean strain rate of  $5 \times 10^{-4} \text{ s}^{-1}$ . Conventional tensile curves are shown on Fig. 4 and conventional tensile properties (yield stress at 0.2% plastic strain  $Y_S$ , ultimate tensile strength UTS, elongation at the onset of necking / maximal load  $A_m$  and elongation at fracture  $A_r$ ) are summarized in Tab. 2. Tests performed at 330°C on specimens irradiated at about 330°C indicate an overall saturation of mechanical properties for doses higher than about 14dpa, although two specimens (3C-TR7 and 3C-TRH1) have a slightly higher yield

stress. The comparison between specimens 1C-TR2, 3C-TR7 and 1H-TR9 shows unexpectedly an effect on the irradiation temperature, with lower yield stress / mechanical strength at lower temperature. The tensile properties of specimens 3C-TR7 and 3C-TRH1, which differs from the geometry of the samples, are very similar, indicating an absence of effect of the sample geometry (in the range considered) on tensile properties of highly irradiated austenitic stainless steels. Specimen 1A-TR9 was found to have tensile properties similar to unirradiated 304 steel, although the irradiation dose was estimated to be higher than 3dpa. Such result is consistent with TEM observations (not shown) showing only few irradiation defects and raises questions about the dose estimation, especially for the upper and lower part of the baffle where flux gradients are expected. Snapshot of the tensile test at 330°C (Fig. 5a) shows a strong necking associated with very large local strains, with a final failure through the appearance of a shear band (Fig. 5b). Tests performed at room temperature are shown on Fig 4b for two specimens with similar irradiation dose and temperature. A very good reproducibility of the tests is observed, showing early necking (defined as a drop of the load), followed by a stress plateau and final hardening behavior up to fracture. Yield stress and mechanical strength are significantly higher than the ones measured at 330°C. Snapshot of the tensile test (Fig. 6a) indicates that the stress plateau corresponds to the propagation of a stable neck along the gage length of the sample. Hardening behavior starts at the end of the propagation of the stable neck, and final fracture surface is perpendicular to the tensile axis (Fig. 6b).

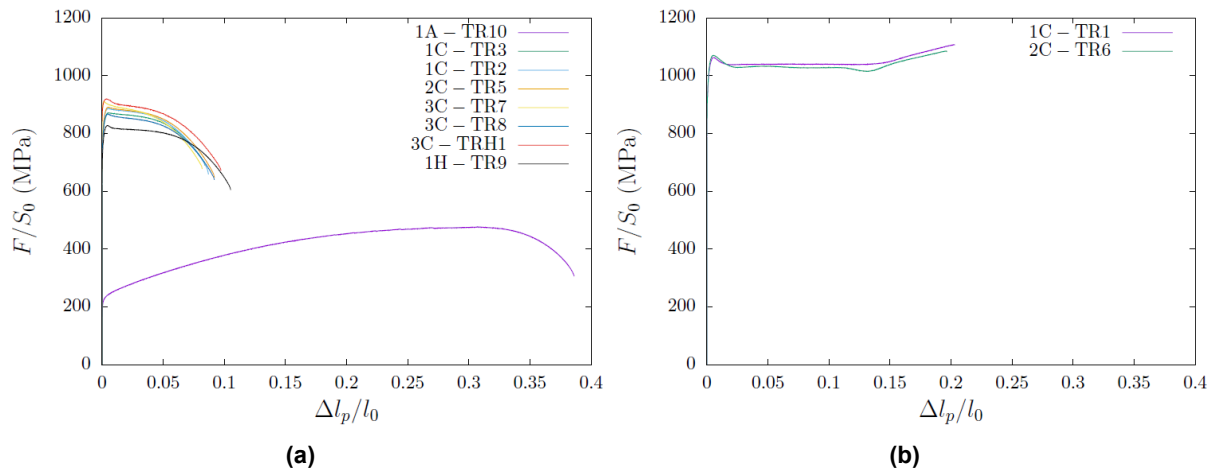


Figure 4: Conventional tensile curves: Conventional stress as a function of conventional plastic strain (a) at 330°C and (b) at room temperature

Specimen	Geometry	Dose (dpa)	$T_{irr}$ (°C)	$T_{test}$ (°C)	YS (MPa)	UTS (MPa)	$A_m$ %	$A_r$ %
1C-TR3	M1	~24	~328	330	839	872	0.53	8.42
1C-TR2	M1	~34	~328	330	859	887	0.52	8.70
2C-TR5	M1	~24	~329	330	861	891	0.53	9.19
3C-TR7	M1	~30	~331	330	910	911	0.15	8.19
3C-TR8	M1	~14	~331	330	843	868	0.49	9.18
3C-TRH1	M2	~30	~331	330	915	920	0.39	9.73
1H-TR9	M1	~31	~300	330	806	828	0.46	10.52
1A-TR10	M1	~3	~325	330	230	477	30.89	38.62
1C-TR1	M1	~24	~328	20	1020	1108	20.30	20.30
2C-TR6	M1	~25	~329	20	1032	1086	19.66	19.66

Table 2: Conventional tensile properties as a function of irradiation dose, irradiation temperature  $T_{irr}$ , and test temperature  $T_{test}$ : yield stress at 0.2% plastic strain YS, ultimate tensile strength UTS, plastic elongation at the onset of necking / maximal load  $A_m$  and plastic elongation at fracture  $A_r$

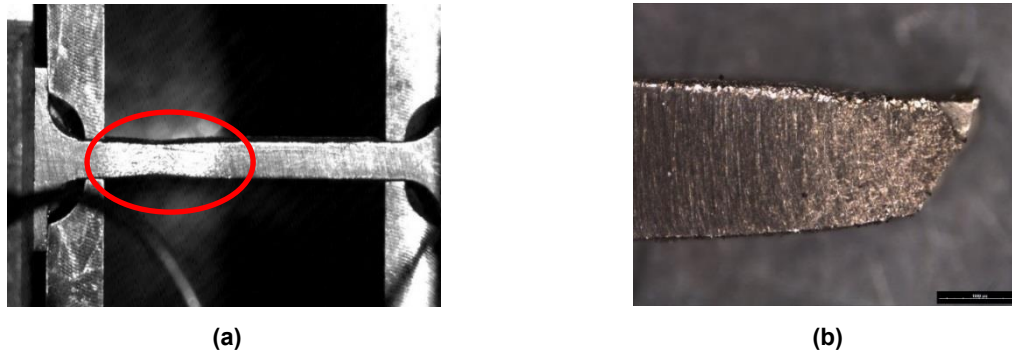


Figure 5: Tensile specimen 3C-TR7 (~30dpa) tested at 330°C: (a) Necking observed during the tensile test, (b) Side view of the fracture surface

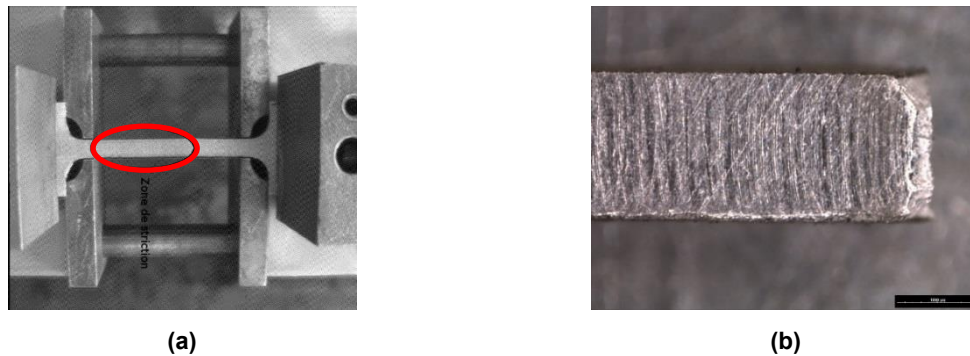


Figure 6: Tensile specimen 2C-TR6 (~25dpa) test at RT: (a) Stable neck propagation observed during the tensile test, (b) Side view of the fracture surface

### Fracture properties

1/2T Compact Tension specimens were precracked in fatigue at room temperature ( $f=5\text{Hz}$ ,  $\Delta K_{\text{ini}} = 18\text{MPa}\sqrt{\text{m}}$ ,  $K_{\text{max}}/K_{\text{min}}=0.25$ ,  $C_g=\ln(\Delta K_{\text{fin}}/\Delta K_{\text{ini}})/(a_f-a_0)=-0.38$ ). Crack length monitoring was performed through compliance technique with an extensometer measuring the Crack Mouth Opening (CMOD) along the load-line of the sample. Depending on the specimen, more than 30k up to 120k cycles were necessary for the crack to reach a targeted  $a_0/W$  ratio of 0.6 ( $a_0 \approx 15\text{mm}$ ). Fracture toughness tests were performed in a furnace at 330°C under Argon flow. Except for specimen 2C-CT7, a crosshead displacement speed of 0.8mm/min was applied (corresponding roughly to 0.16mm/min of CMOD speed at the end of the test), with hold time of 30s every 20 $\mu\text{m}$  displacement followed by partial discharge (15% of the hold time load) of the specimen and reloading. Due to very limited stable crack growth, compliance technique was not used to estimate the crack length during the test. Instead, tests were stopped shortly after the peak load, and samples were cooled down to room temperature and finally cracked in fatigue. Load vs. Crack Mouth Opening Displacement are given in Fig. 7, showing a good reproducibility of the tests. Two of the seven CT specimens (not reported in Fig. 7) were found to have initial fatigue crack slanted, preventing using them to evaluate fracture toughness with standardized methods. The five other CT specimens have relatively straight crack front: initial fatigue crack length and stable crack growth were measured through nine-point measurements (see Fig. 8), and the corresponding J values were computed according to ASTM1820 [7]. For each test, the initial crack length, stable crack growth and associated J (and K according to  $K=\sqrt{EJ/(1-\nu^2)}$ , with  $E=200\text{GPa}$  and  $\nu=0.3$ ) values are given in Tab. 3.

Specimen	Dose (dpa)	B (mm)	B <sub>N</sub> (mm)	W (mm)	a <sub>0</sub> (mm)	a <sub>f</sub> (mm)	Δa (mm)	J (kJ/m <sup>2</sup> )	K (MPa√m)
2C-CT8	~15	12.25	9.66	24.79	14.07	15.28	1.21	38	91
2C-CT4	~15	12.56	9.64	24.76	13.74	14.23	0.49	37	90
1C-CT9	~15	12.21	9.56	24.71	14.48	14.70	0.22	37	90
2C-CT7	~32	12.34	9.62	24.75	14.65	14.65	-	38	91
2C-CT3	~32	12.49	9.95	25.90	14.80	15.28	0.48	24	73

Table 3: Results of the fracture toughness tests at 330°C: Geometry of the 1/2T CT specimens (Thickness B and net thickness between the side grooves B<sub>N</sub>, width W, fatigue crack length a<sub>0</sub>, final crack length a<sub>f</sub> and propagation Δa= a<sub>f</sub> - a<sub>0</sub>), J-integral value (and stress intensity factor) for the given crack propagation

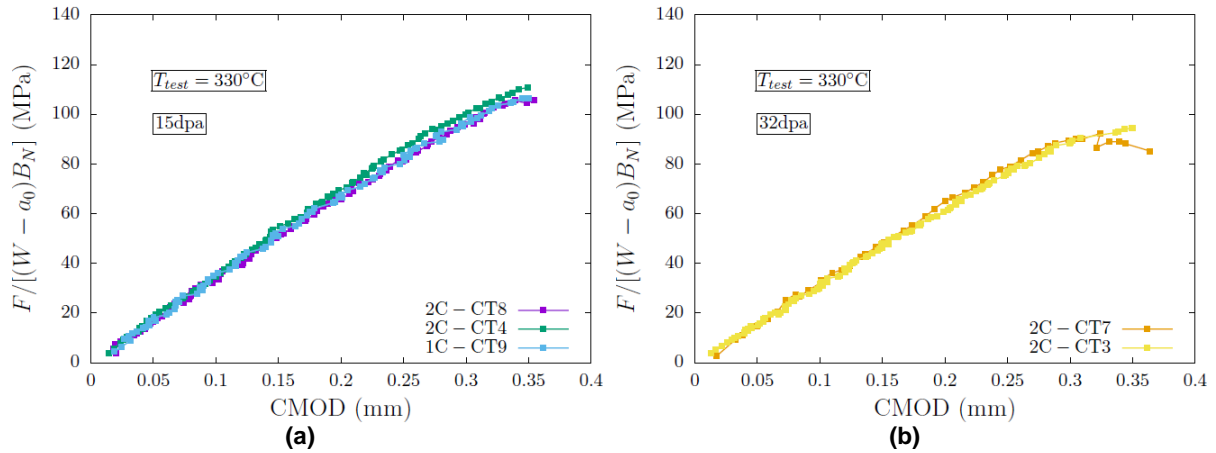


Figure 7: Load (normalized by the remaining ligament section) as a function of Crack Mouth Opening Displacement (CMOD) for fracture toughness tests at 330°C for (a) 15dpa and (b) 32dpa samples.

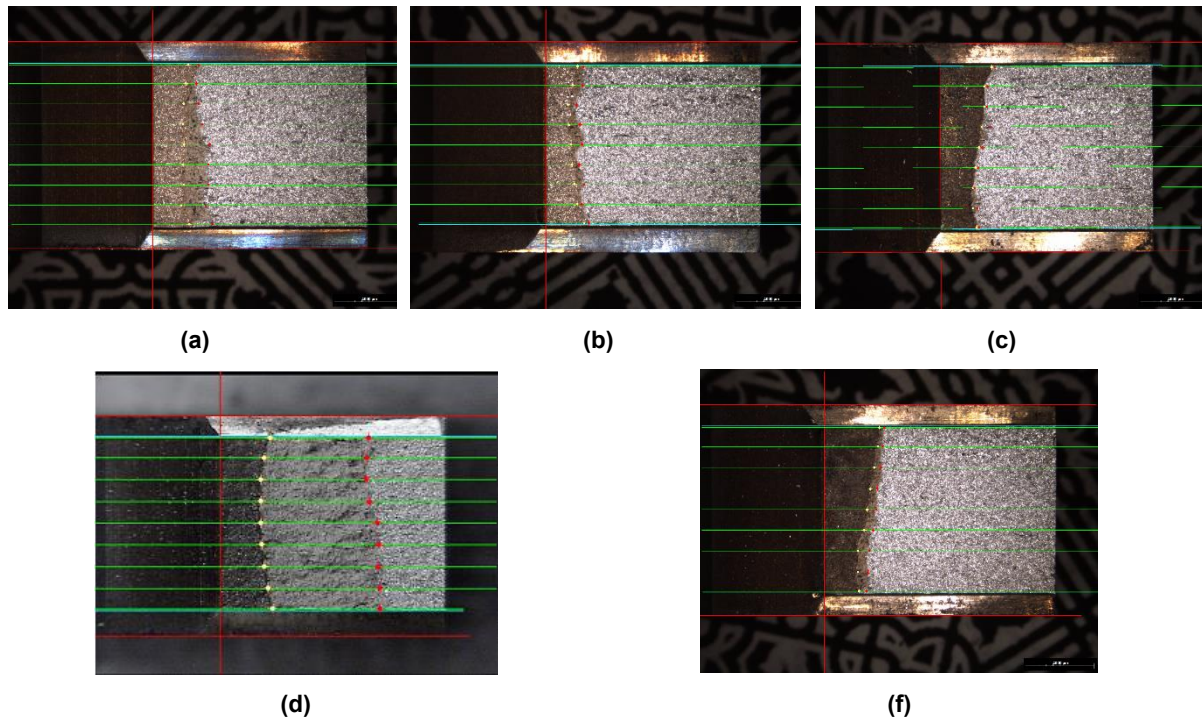


Figure 8 : Fracture surfaces of samples (with nine points crack measurements) (a) 2C-CT8, (b) 2C-CT4, (c) 1C-CT9, (d) 2C-CT7 and (e) 2C-CT3. Three different regions can be observed on each fracture surface characterized by their different colors (and delimited with yellow and red dots): initial fatigue crack, crack propagation during the toughness test, and final fatigue cracking, from left to right

For the specimens irradiated up to 15dpa, normalized load vs. CMOD curves are very reproducible (Fig. 7a), and three different values of crack growth were obtained (Fig. 8a,b,c), allowing plotting an estimate of the J-da curve, under the assumption that the three specimens have the same fracture resistance (Fig. 9). Tearing modulus appears to be close to zero, so that J (of K) values reported can be considered as close to initiation values. For the specimens irradiated at 32dpa, only one of them (2C-CT3) was interrupted during the stable crack growth phase, while unstable crack growth occurred for the other (2C-CT7). Estimation of initiation J-integral for the latter was performed assuming crack started to propagate at the peak load. Fracture toughness evaluations at 15dpa are found to be very reproducible for the material used, leading to values close to  $90\text{MPa}\sqrt{\text{m}}$ . A slight decrease of fracture toughness with irradiation between 15dpa and 32dpa is observed, down to minimal value of  $73\text{MPa}\sqrt{\text{m}}$ .

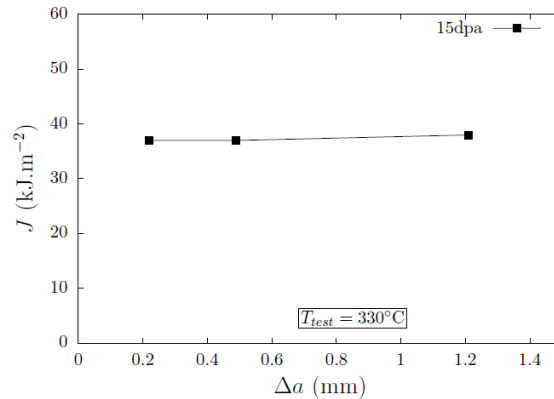


Figure 9 : J-da curve obtained from interrupted tests at 330°C on three 1/2T CT specimens irradiated to 15dpa.

### SEM observations

Fracture surfaces of tensile specimens 2C-TR5 (tested at 330°C) and 2C-TR6 (tested at 20°C) were observed with Scanning Electron Microscope (SEM), under secondary electron mode. At 330°C (Fig. 10), the fracture surface is characterized by the presence of dimples of various sizes and shapes, indicating a void growth to coalescence fracture mechanism. Depending on the location of the fracture surfaces, equiaxed or elongated dimples are observed, correlated a priori with the local orientation of the fracture surface with the tensile axis. When the local fracture surface is parallel to the loading axis, dimples are mostly equiaxed while they are elongated in regions where the fracture surface is tilted with respect to the loading axis. At lower magnification, the presence of elongated dimples corresponds to regions appearing mostly flat. Two populations of dimple sizes can be observed, the large one being of about 5 microns diameter often associated with spherical precipitates inside, while the second population has dimples less than 1 micron diameter often free of precipitates. Fracture surface of the specimen tested at room temperature (Fig. 11) shows a large region located at the middle of the specimen which is perpendicular to the tensile axis and almost completely intergranular in nature, while an external layer, slanted, is transgranular. Images at different magnifications of the intergranular region are shown in Fig. 11b,c,d. Numerous intergranular cracks can be observed, indicating that the fracture mechanism at room temperature on tensile specimen may not correspond to the propagation of a single (intergranular) crack, but should be considered rather to a coalescence process of multiple intergranular cracks. Inside the intergranular region, few regions with dimples are observed that are surrounded by intergranular facets, as well as cracked or debonded precipitates. The intergranular or transgranular nature of the ductile region is however difficult to assess. The external layer of the fracture surface is fully ductile, characterized by the presence of dimples similar to what has been already described for the specimen tested at 330°C, with two different dimple sizes population. SEM observations of CT specimens fracture surfaces are in progress, and will be reported elsewhere.

### Discussion

The evolution of tensile properties (yield stress and ultimate tensile strength) are plotted as a function of dose in Fig. 12, considering the available data in the literature and results obtained in this study, and restricting to 304(L) materials irradiated in LWR conditions. The MRP correlation curves [3] for solution-annealed austenitic stainless steels (304(L), 347) irradiated and tested at temperature close to 330°C, and referred to as MRP2004, are also compared to the data. As discussed in [1], most of the data used to get the MRP2004 curves comes from materials irradiated in fast reactors, which, albeit following the same trends than materials irradiated in LWR conditions, might not be quantitatively representative of the latter. This is confirmed by the additional data provided in this study that are significantly harder (about 50MPa) than the predictions of MRP curves, for both yield stress and ultimate tensile strength. New (almost upper-bound) fitting curves are proposed to describe the hardening of 304(L) materials under LWR conditions irradiated and tested at a temperature close to 330°C. Less data are available for 304(L) materials irradiated in LWR conditions at a temperature close to 330°C but tested at room

temperature. Results are given in Fig. 12(c,d) with proposition of (almost upper-bound) fitting curves.

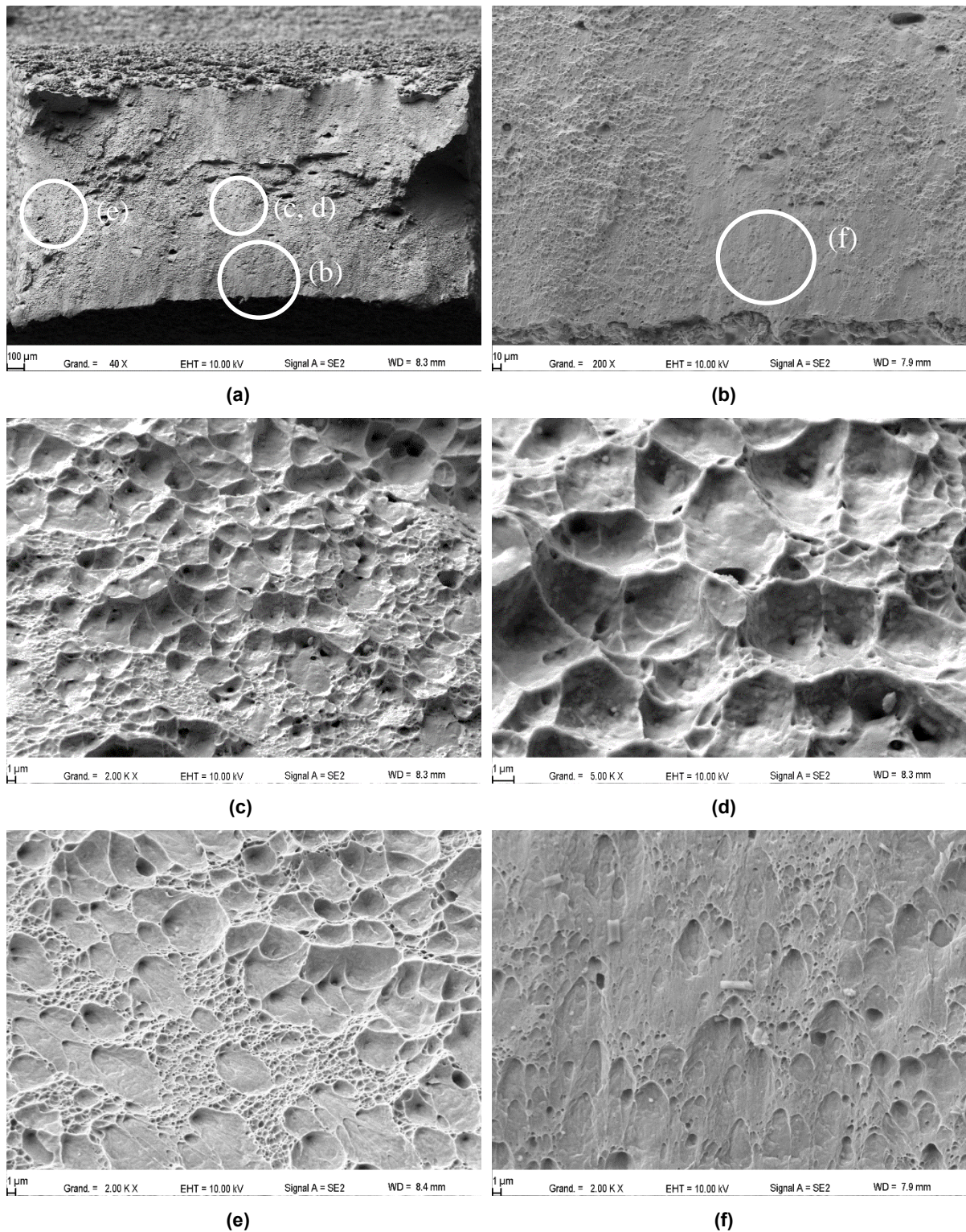


Figure 10: SEM fracture surface observations of tensile specimen 2C-TR5 (~24dpa) tested at 330°C

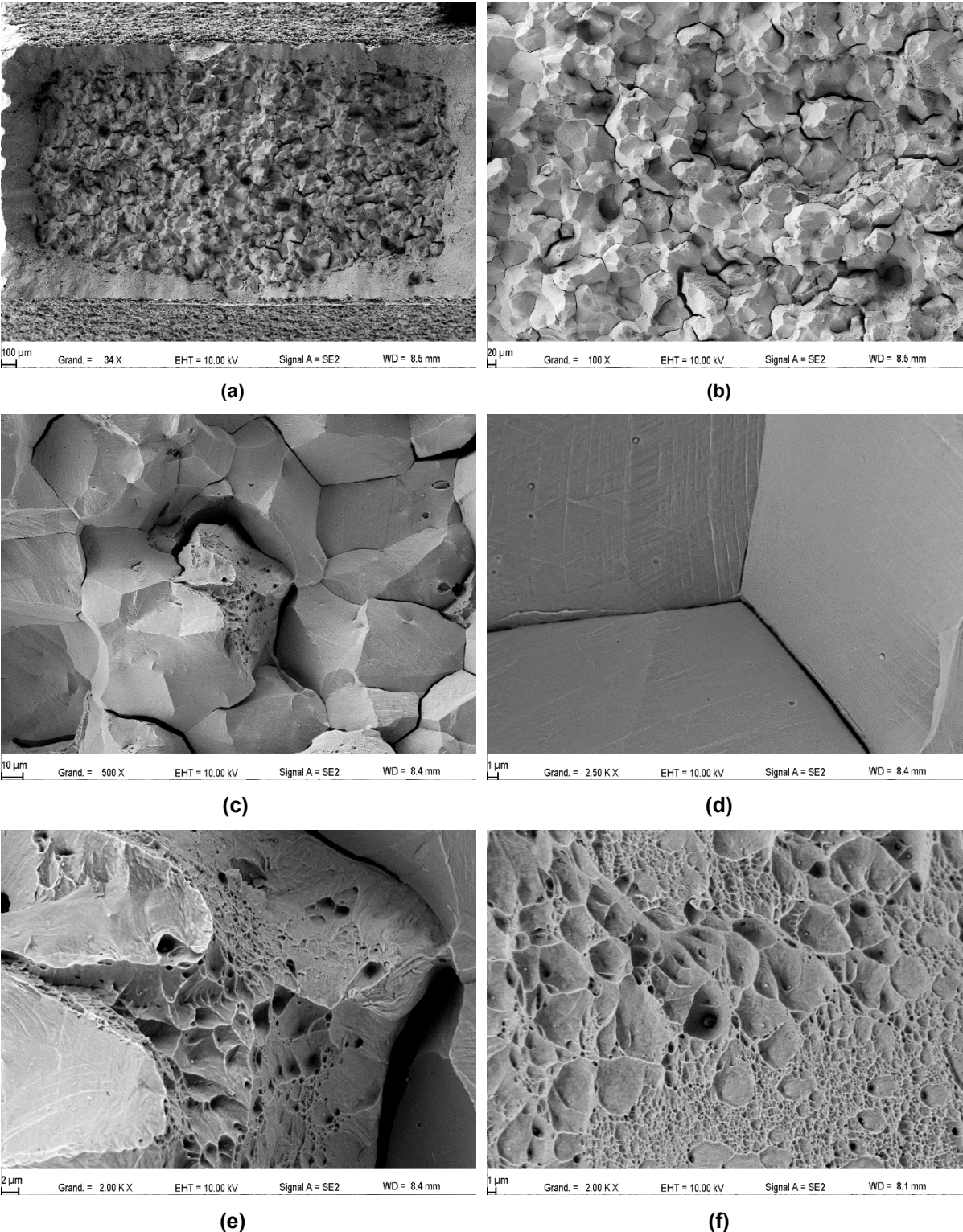
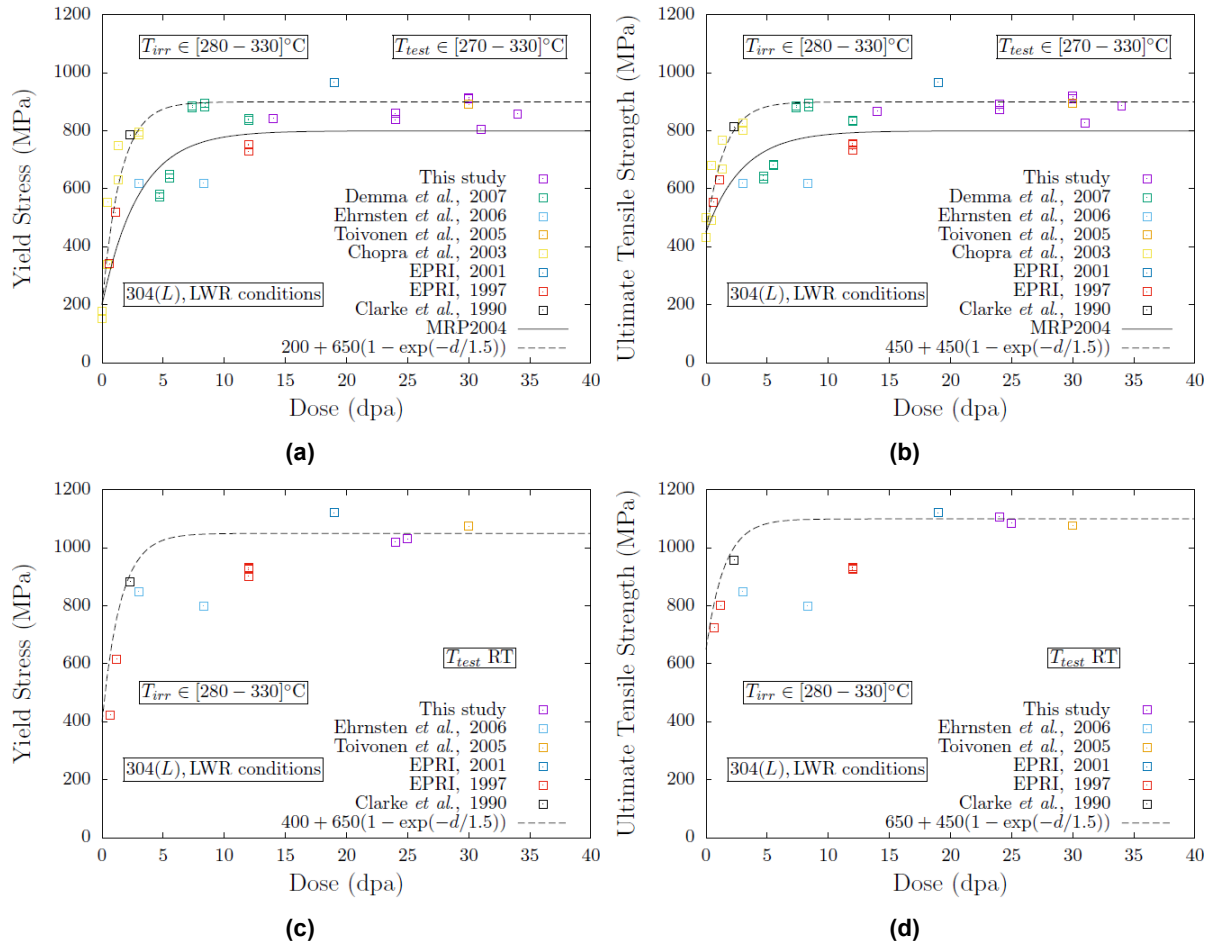


Figure 11: SEM fracture surface observations of tensile specimen 2C-TR6 (~24dpa) tested at 20°C



**Figure 12: Evolution of yield stress and ultimate tensile strength for 304(L) materials under LWR irradiation conditions, and tested at a temperature close to 330°C (a,b) or at room temperature (c,d).**

Fracture surfaces of tensile specimens shown on Fig. 10 and 11, tested at 330°C and RT respectively, are fully consistent with observations obtained for the same material in [10], as well as with critical assessment of fracture observations provided in [4]. In particular, the fully dimpled surface of the specimen tested at 330°C – without any occurrence of channel fracture - indicate that, for 304(L) materials irradiated in LWR conditions up to high doses, classical models of ductile fracture based on void growth to coalescence could be used to predict failure, at least for the mechanical loading conditions obtained in tensile tests. SEM observations of CT specimens tested at 330°C are in progress, and would allow extending this statement to mechanical loading conditions relevant to crack-tip. Specimen tested at room temperature exhibits both stable necking propagation and (almost-) fully intergranular fracture. It has been proposed in [4,17] that both observations could be rationalized by the fact that a martensitic transformation occurred, which remains to be assessed in our study through TEM observations.

Comparisons of fracture toughness estimations of 304(L) materials irradiated in LWR conditions to high doses (> 4dpa) are shown on Fig. 13. Considerable scatter are observed, resulting from metallurgical reasons (as in [8] associated with the presence of stringers) or that may result from significant differences in tensile properties (as for the data in [9] that have rather low yield stress and ultimate tensile strength compared to other materials irradiated to similar doses). Fracture toughness evaluation obtained in this study are within the scatter of previous available data. A slight decrease of fracture toughness is observed between 15dpa and 32dpa that would require further experimental data at higher doses for materials irradiated in LWR conditions to assess to absence of additional embrittlement.



- 8) A. Demma et al., "Fracture toughness of highly irradiated stainless steels in boiling water reactors", 13<sup>th</sup> International Conference on Environmental Degradation of Materials in Nuclear Systems – Water Reactors, 2007, Whistler, B.C., Canada.
- 9) U. Ehrnsten et al., "Fracture toughness of stainless steels irradiated up to ~9dpa in commercial BWRs", 6<sup>th</sup> International Symposium on Contribution of Materials Investigations to improve the Safety and Performances of LWRs, 2006, Fontevraud, France.
- 10) A. Toivonen et al., "Fractographic observations on a highly irradiated AISI 304 steel after constant load tests in simulated PWR water and argon after supplementary tensile and impact tests", 12<sup>th</sup> International Conference on Environmental Degradation of Materials in Nuclear Systems – Water Reactors, 2005, Salt Lake City, USA.
- 11) O.K. Chopra et al., "Fracture Toughness and Crack Growth Rates of Irradiated Austenitic Stainless Steels," Argonne National Laboratory for U.S. Nuclear Regulatory Commission, NUREG/CR-6826, 2003.
- 12) Materials Reliability Program, Hot Cell Testing of Baffle/Former Bolts Removed from Two Lead PWR Plants (MRP-51), EPRI Technical Reports, 1003069, 2001
- 13) VTT (Technical Research Center of Finland) *BWR Vessel and Internals Project: Fracture Toughness and Tensile Properties of Irradiated Austenitic Stainless Steel Components Removed From Service (BWRVIP-35)*, Electric Power Research Institute (EPRI), Palo Alto, CA: June 1997. EPRI TR-108279.
- 14) W.L. Clarke et al., "Evaluation of the Fracture Toughness of Irradiated Stainless Steel Using Short Rod Specimens," Effects of Radiation on Materials:14th International Symposium, Philadelphia, 1990, USA.
- 15) M. L. Herrera et al., "Evaluation of The Effects of Radiation on the Fracture Toughness of BWR Components," International Conference on Nuclear Engineering (ICONE-4), Volume 5, pp. 245-251, ASME 1996.
- 16) Materials Reliability Program. Fracture Toughness Testing of Decommissioned PWR Core Internals Materials Samples (MRP-160). EPRI Technical Reports, 1012079, 2005
- 17) B. Margolin et al., "The radiation swelling effect on fracture properties and fracture mechanisms of irradiated austenitic steels. Part I: Ductile and fracture toughness, J. Nuc. Mat. 480, 52-68 (2016)